

## MYELOID NEOPLASIA

## Rare and private spliceosomal gene mutations drive partial, complete, and dual phenocopies of hotspot alterations

Joseph Pangallo,<sup>1,2</sup> Jean-Jacques Kiladjian,<sup>3</sup> Bruno Cassinat,<sup>3</sup> Aline Renneville,<sup>4</sup> Justin Taylor,<sup>5</sup> Jacob T. Polaski,<sup>1,2</sup> Khrystyna North,<sup>1,2,6</sup> Omar Abdel-Wahab,<sup>5</sup> and Robert K. Bradley<sup>1,2,6</sup>

<sup>1</sup>Computational Biology Program, Public Health Sciences Division, and <sup>2</sup>Basic Sciences Division, Fred Hutchinson Cancer Research Center, Seattle, WA; <sup>3</sup>Assistance Publique–Hôpitaux de Paris and INSERM Unité Mixte de Recherche en Santé 1131, Institut Universitaire d'Hématologie, Hôpital Saint-Louis, Paris, France; <sup>4</sup>Hematology Laboratory, Biology and Pathology Center, Centre Hospitalier Universitaire, Lille, France; University of Lille Nord de France, Lille, France; UMR-S 1172, Team 3, Cancer Research Institute of Lille, Lille, France; <sup>5</sup>Human Oncology and Pathogenesis Program and Leukemia Service, Memorial Sloan Kettering Cancer Center, New York, NY; and <sup>6</sup>Department of Genome Sciences, University of Washington, Seattle, WA

## KEY POINTS

- A subset of patients with hematologic malignancies carry rare spliceosomal gene mutations of unknown disease relevance.
- Many rare and even private spliceosomal gene mutations create molecular phenocopies of hotspot mutations and are likely pathogenic.

**Genes encoding the RNA splicing factors *SF3B1*, *SRSF2*, and *U2AF1* are subject to frequent missense mutations in clonal hematopoiesis and diverse neoplastic diseases. Most “spliceosomal” mutations affect specific hotspot residues, resulting in splicing changes that promote disease pathophysiology. However, a subset of patients carries spliceosomal mutations that affect non-hotspot residues, whose potential functional contributions to disease are unstudied. Here, we undertook a systematic characterization of diverse rare and private spliceosomal mutations to infer their likely disease relevance. We used isogenic cell lines and primary patient materials to discover that 11 of 14 studied rare and private mutations in *SRSF2* and *U2AF1* induced distinct splicing alterations, including partially or completely phenocopying the alterations in exon and splice site recognition induced by hotspot mutations or driving “dual” phenocopies that mimicked 2 co-occurring hotspot mutations. Our data suggest that many rare and private spliceosomal mutations contribute to disease pathogenesis and illustrate the utility of molecular assays to inform precision medicine by inferring the potential disease relevance of newly discovered mutations. (*Blood*. 2020;135(13):1032-1043)**

## Introduction

Somatic mutations in genes encoding RNA splicing factors are among the most common genetic changes observed in many hematologic malignancies.<sup>1-6</sup> Also recurrently observed in solid tumors, albeit at lower frequencies, these spliceosomal mutations occur most commonly in *SF3B1*, *SRSF2*, and *U2AF1* as missense changes at a highly specific set of hotspot residues.<sup>7,8</sup> Hotspot mutations in *SF3B1*, *SRSF2*, and/or *U2AF1* are observed in many patients with myelodysplastic syndromes and related hematologic diseases, and occur at high frequencies of from 5% to 18% in chronic lymphocytic leukemia,<sup>5,6,9,10</sup> 5% to 25% of acute myeloid leukemia (AML) in adults,<sup>11</sup> and 14% to 29% in uveal melanoma.<sup>12,13</sup>

Consistent with the frequent and recurrent nature of spliceosomal mutations, functional studies indicate that these lesions drive disease. Mutations in *SRSF2* and *U2AF1* specifically occur at high rates in elderly subjects with clonal hematopoiesis and confer a high risk for transformation to overt myeloid leukemia in this setting.<sup>14,15</sup> In many cases, concrete links among altered RNA splicing, specific target genes, and hallmark disease phenotypes have been identified. For example, *SF3B1* mutations

alter RNA branchpoint recognition to cause *BRD9* mis-splicing and cell transformation,<sup>16-19</sup> *SRSF2* mutations alter exonic splicing enhancer recognition to cause *EZH2* mis-splicing and impaired hematopoiesis,<sup>20,21</sup> and *U2AF1* mutations alter 3' splice site recognition to cause *IRAK4* mis-splicing and aberrant innate immune signaling.<sup>22-24</sup>

Although the bulk of *SF3B1*, *SRSF2*, and *U2AF1* mutations affect a small set of hotspot residues, a minority of patients carry non-hotspot mutations, some of which are recurrent despite their relative rarity. The relevance of rare and private (observed in only 1 patient) spliceosomal lesions to disease is unclear, but they are enriched in hematologic malignancies, preferentially occur as missense changes, and appear in a heterozygous genetic context, similar to their hotspot counterparts (Figure 1A-B).<sup>25</sup> This situation, in which a cancer-relevant gene is subject to hotspot mutations of known significance, as well as rare or private mutations of unknown functional consequence, is not unique to splicing factors. Rare and private mutations have frequently been ignored in favor of their more common hotspot counterparts because of the inherent challenges of studying a diverse mutational spectrum. However, advances in molecular and functional

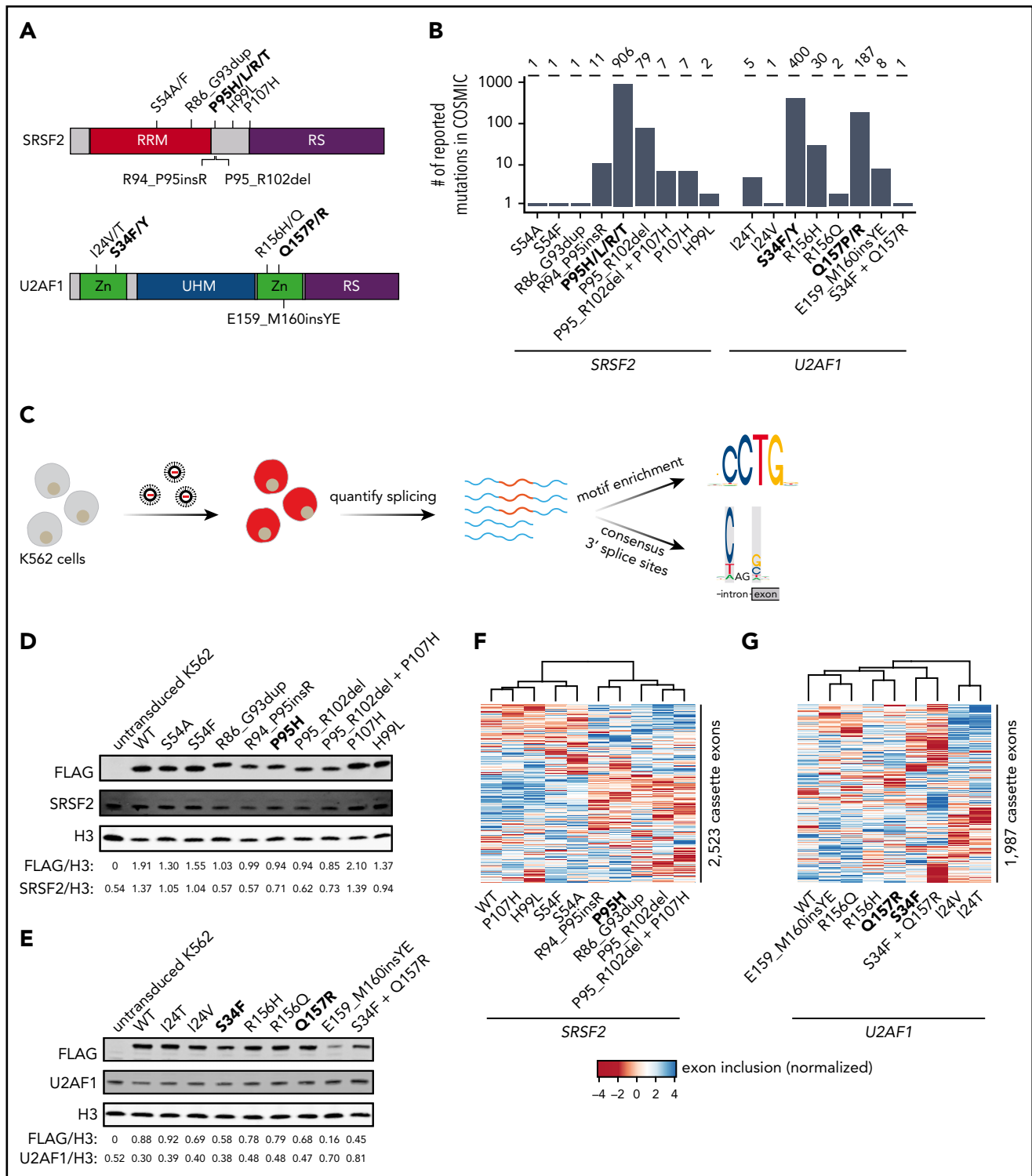


**Figure 1. Strategy for classification of rare, non-hotspot SRSF2 and U2AF1 mutations.** (A) Hotspot (bold) and select rare and private mutations affecting SRSF2 and U2AF1. RRM, RNA recognition motif; RS, arginine/serine-rich domain; UHM, U2AF1 homology motif; Zn, zinc finger domain. (B) Numbers of reported mutations in SRSF2 and U2AF1 in the Catalogue of Somatic Mutations in Cancer (COSMIC) database as of 17 September 2018. SRSF2S54A was identified in a patient sample, but is not present in COSMIC. (C) Schematic of our strategy for transgenically expressing individual mutations in cell culture and performing subsequent transcriptome analyses. (D) Western blot for FLAG, SRSF2, and Histone H3 (H3), using lysate from untransduced K562 cells or K562 cells that stably expressed FLAG-tagged WT or mutant SRSF2 (mutation indicated earlier). H3 is a loading control. FLAG and SRSF2 band intensities were quantified using ImageJ and normalized to the respective band intensity for H3. (E) As in panel D, but for U2AF1. (F-G) Heat map and associated dendrogram representing an unsupervised cluster analysis based on cassette exon inclusion levels computed from the transcriptomes of K562 cells stably expressing the indicated alleles of SRSF2 (F) or U2AF1 (G). Exon inclusion values were z-score normalized.

assays have enabled recent studies to identify protumorigenic roles of rare and even private inherited genetic variants and somatically acquired mutations of previously unknown significance in *BRCA1*, *EGFR*, *KRAS*, and other cancer-relevant genes.<sup>26-30</sup> Each of those studies relied on a different approach to classification (eg, measuring how each rare variant or mutation affected biochemical activity [*BRCA1*], gene expression profiles [*EGFR* and others], or tumor outgrowth [*KRAS* and others]), selected based on known molecular or biological consequences of hotspot mutations.

Here, we conducted a systematic study to infer the likely disease relevance of rare and private mutations in *SRSF2* and *U2AF1*. Our study was motivated in part by a recent report of 3 patients with chronic lymphocytic leukemia with novel *SF3B1* in-frame deletions whose splicing profiles mimicked those of patients with hotspot *SF3B1* mutations,<sup>31</sup> as well as our recent finding that both rare and common *SF3B1* mutations converge on *BRD9* mis-splicing across cancer types.<sup>19</sup> We wondered whether rare and private *SRSF2* and *U2AF1* mutations might similarly mimic the splicing phenotypes of hotspot mutations, which induce highly specific alterations in exon or 3' splice site recognition that drive key disease phenotypes.<sup>20-24</sup> We hypothesized that rare or private *SRSF2* and *U2AF1* mutations that phenocopied hotspot-induced changes in splicing were candidate drivers, whereas mutations that induced few or no splicing changes were likely passengers. We used this approach in both isogenic cell lines and primary patient materials to infer the likely pathogenicity of non-hotspot *SRSF2* and *U2AF1* mutations (Figure 1C).

## Methods

### Vector construction and cell line production

An insert containing *SRSF2* (or *U2AF1*) cDNA-FLAG-P2A-mCherry was cloned into the lentiviral vector pRRLSIN.cPPT.PGK-GFP.WPRE (Addgene plasmid 12252). Mutations in *SRSF2* or *U2AF1* were then created by site-directed mutagenesis. These plasmids were cotransfected with psPAX2 (Addgene plasmid 12260) and envelope vector pMD2.G (Addgene plasmid 12259) into 293T cells. Lentivirus was collected from the supernatant 48 hours post-transfection. Stable cell lines were made by transducing K562 cells with lentivirus at a multiplicity of infection of 2.5 (*U2AF1*) or 5 (*SRSF2*). Cells were expanded, and mCherry<sup>+</sup> cells were collected by fluorescence-activated cell sorting. K562 cells were cultured in Iscove modified Dulbecco medium supplemented with 10% fetal bovine serum.

### Western blotting

Protein lysates were extracted from K562 cells by resuspension in radioimmunoprecipitation assay (RIPA) buffer. Thirty micrograms of protein were then loaded for sodium dodecyl sulfate-polyacrylamide gel electrophoresis and transferred to a nitrocellulose membrane. Proteins were probed with the following antibodies: anti-*U2AF1* (A302-080A; Bethyl Laboratories), anti-*SRSF2* (04-1550; MilliporeSigma), anti-FLAG (MA1-91878; Thermo Fisher Scientific), and anti-Histone H3 (ab179; Abcam1).

### RNA-seq library preparation and analysis

Total RNA was isolated from K562 cells or patient materials, using the TRIzol reagent (Thermo Fisher Scientific). Four micrograms (K562) or 500 ng (patient materials) of total RNA was used as to

make poly(A)-selected, unstranded libraries with the TruSeq RNA Library Prep Kit v2 (Illumina). Purified libraries were sequenced on the Illumina Hi-Seq 2000 with 2 × 50-bp reads.

After RNA-seq read mapping, isoform expression levels were estimated as previously described.<sup>23</sup> Unless otherwise specified, a splicing event was classified as differentially spliced if it exhibited a change in isoform ratio of at least 10% and a Bayes Factor of at least 5. Wagenmakers's framework<sup>32</sup> was used to compute Bayes factors associated with differences in isoform ratio between samples. A full description of the analysis can be found in supplemental Methods, available on the *Blood* Web site.

### Primary human samples

Studies were approved by the Institutional Review Boards of Memorial Sloan Kettering Cancer Center (MSK; under MSK Institutional Review Board protocol 06-107) and the Hôpital Saint-Louis, and conducted in accordance with the Declaration of Helsinki protocol. Written informed consent was obtained from all participants. Patient samples were anonymized by the Hematologic Oncology Tissue Bank of MSK and the Hôpital Saint-Louis. Mutational analysis of *SRSF2* and *U2AF1* was performed on genomic DNA from bone marrow mononuclear cells by targeted sequencing using MSK Heme-PACT assay<sup>33</sup> (for samples from MSK).

### Data availability

RNA-seq data generated as part of this study were deposited in the Gene Expression Omnibus (accession number GSE135732). Previously published data were downloaded from the Gene Expression Omnibus under accession numbers GSE65349,<sup>20</sup> GSE114922,<sup>34</sup> GSE66917, and GSE67039.<sup>35</sup> TCGA data were downloaded from CGHub.<sup>36,37</sup>

## Results

### Diverse *SRSF2* and *U2AF1* mutations alter RNA splicing programs

We queried the Catalogue of Somatic Mutations in Cancer database<sup>25</sup> to identify all *SRSF2* and *U2AF1* mutations with confirmed somatic status as of 17 September 2018. We selected 8 *SRSF2* and 6 *U2AF1* representative non-hotspot mutations for detailed study (Figure 1B). These mutations exhibited highly variable frequencies (ranging from private to common), represented both missense changes and indels (insertions and deletions), and were present as either single polymorphisms or indels, as well as more complex events (involving multiple mutations, such as *U2AF1S34F\_Q157R*, for which 2 hotspot mutations co-occurred on the same allele). We systematically determined how each mutation affected RNA splicing in both engineered cell lines and primary patient materials, when available, as follows.

We first established cell culture models of each selected *SRSF2* and *U2AF1* mutation. We modeled each mutation via transgenic expression in K562 cells for 2 reasons. First, spliceosomal mutations are always coexpressed with a wild-type (WT) allele, which is required for cell survival.<sup>38</sup> Our lentiviral construct contained a fluorescent marker that permitted titration of transgene expression by flow sorting, which was critical, given previous reports that

the ratio of mutant to WT protein controls global missplicing profiles.<sup>39</sup> Second, we and others have previously demonstrated that simultaneous expression of a transgenic mutant protein and endogenous WT protein in K562 cells faithfully recapitulates mis-splicing profiles observed in primary patient materials with *SRSF2* or *U2AF1* mutations.<sup>20,23,40</sup>

We transduced K562 cells with a lentiviral construct expressing each mutant cDNA (individually) and established stable transgenic cell lines for each selected mutation (Figure 1C; supplemental Figure 1). We additionally established cell lines expressing transgenic WT *SRSF2* or *U2AF1* as a control for transgene expression, as well as cell lines expressing the hotspot mutations *SRSF2P95H*, *U2AF1S34F*, and *U2AF1Q157R*. We modeled 2 different *U2AF1* hotspot mutations because we previously found that mutations affecting *U2AF1*'s first vs second zinc finger result in distinct alterations in 3' splice site recognition.<sup>23</sup> We confirmed that transgene introduction resulted in relative levels of mutant vs WT *SRSF2* and *U2AF1* mRNA within physiological ranges observed in patients and that each cell line expressed mutant protein in the absence of significant perturbations to total (mutant + WT) levels of *SRSF2* or *U2AF1* relative to untransduced cells (Figure 1D-E; supplemental Figure 2).

We first tested whether expressing rare *SRSF2* and *U2AF1* mutations altered global splicing programs. We performed high-coverage RNA-seq on each of the 19 distinct cell lines and quantified global isoform expression for ~125 000 alternative splicing events and aberrant retention or splicing of ~160 000 constitutive introns, as previously described.<sup>41</sup> An unsupervised cluster analysis based on cassette exon inclusion, where we focused on cassette exons because *SRSF2* and *U2AF1* hotspot mutations primarily affect this category of splicing event,<sup>20,23</sup> revealed allele-specific clustering that was distinct from WT splicing programs in many cases (Figure 1F-G). This simple analysis suggested that at least some rare mutations influenced splicing programs.

### Rare and hotspot *SRSF2* mutations converge on altered exonic splicing enhancer preference

We sought to determine how rare spliceosomal mutations influenced global splicing programs (Figure 1F). We first focused on *SRSF2* mutations, because all hotspot *SRSF2* mutations affect a single residue (P95) and cause identical alterations in the RNA splicing process.<sup>20,21</sup> Similar to their hotspot counterparts, rare *SRSF2* mutations were associated with a diversity of splicing changes affecting competing splice sites, cassette exons, retained introns, and aberrant splicing or retention of normally constitutive introns, with cassette exons representing the most commonly differentially spliced event. The numbers of significantly differentially spliced events, defined as events with a change in isoform ratio of at least 10% and Bayes factor of at least 5 relative to WT-expressing control cells, varied by an order of magnitude across the different mutations, suggestive of dramatically different functional consequences (Figure 2A; supplemental Table 1).

Hotspot *SRSF2* mutations alter *SRSF2*'s RNA-binding affinity and avidity to induce sequence-specific changes in exonic splicing enhancer (ESE) preference. Although WT *SRSF2* recognizes a consensus motif SSNG (S = G or C) in pre-mRNA, *SRSF2P95H/L/R* mutations promote recognition of C-rich variants and repress recognition of G-rich variants.<sup>20,21,42</sup> We therefore determined

how each rare mutation affected recognition of G- vs C-rich variants of the core SSNG motif. We identified all differentially spliced cassette exons in each cell line (supplemental Figure 3), identified all occurrences of SSNG motifs in each cassette exon, and computed the enrichment for each SSNG motif variant in cassette exons that were promoted vs repressed in mutant vs WT cells. Six of the 8 tested non-hotspot *SRSF2* mutations caused significant alterations in C- vs G-rich ESE preference that were restricted to differentially spliced cassette exons, an identical pattern to that observed for the *SRSF2P95H* hotspot mutation (Figure 2B; supplemental Figure 4). Our approach allowed us to deconvolve complex co-mutation events such as *SRSF2P95\_R102del+P107H*. *SRSF2P95\_R102del* alone phenocopied *SRSF2P95* mutations, whereas *SRSF2P107H* alone had no effect, suggesting that the first lesion might be pathogenic whereas the second is functionally silent (Table 1).

We next confirmed our results in the physiological setting of primary patient materials. We searched for non-hotspot *SRSF2* mutations in institutional biorepositories as well as published cohorts of patients with AML,<sup>20,35</sup> chronic myelomonocytic leukemia,<sup>20</sup> and myelodysplastic syndromes.<sup>34</sup> We identified samples carrying *SRSF2S54A/F*, *SRSF2R94\_P95insR*, and *SRSF2P95\_R102del*; performed RNA-seq or reanalyzed published data when available; and tested for sequence-specific alterations in ESE preference. In each case, we observed enhanced and spatially restricted recognition of C- vs G-rich SSNG motifs that was consistent with our results from cell culture (Figure 2B; supplemental Figure 4). Interestingly, although many non-hotspot mutations induced seemingly complete phenocopies of enhanced recognition of C- vs G-rich ESEs, *SRSF2S54A/F* induced partial phenocopies apparent as decreased recognition of GGNG in the absence of enhanced recognition of CCNG (Table 1; supplemental Figure 4). Unsupervised clustering of K562 cell lines with primary patient samples revealed that global mis-splicing profiles segregated by mechanistic classification, consistent with a central role for altered ESE recognition in driving global mis-splicing programs in cells with rare as well as hotspot *SRSF2* mutations (Figure 2C). We experimentally validated results from RNA-seq by performing reverse transcription polymerase chain reaction (RT-PCR) on 8 distinct mis-splicing events. In each case, the private mutation *SRSF2R86\_G93dup* and the common mutation *SRSF2P95H* induced concordant mis-splicing in K562 cells (Figure 12D-E; supplemental Figure 5).

We next experimentally confirmed that rare *SRSF2* mutations caused aberrant exon recognition in a manner that depended on altered ESE recognition. As we previously demonstrated that enhanced cassette exon recognition in hotspot mutant cells was a result of the presence of CCNG motifs,<sup>20</sup> we here instead tested whether repressed cassette exon recognition was a result of the presence of GGNG motifs. A cassette exon within *RPL21* exhibited significant and consistent repression in mutant cells and also contained a single GGNG motif, making it an ideal system to test this hypothesis (Figure 2F). We cloned this cassette exon and flanking introns into a plasmid, introduced a GGTG>CCTG mutation, and expressed both GGTG (native) and CCTG versions of this minigene in K562 cells. We focused on *SRSF2R86\_G93dup*, a private mutation for which we were unable to identify corresponding patient materials but that phenocopied hotspot mutations in cell culture, as well as the rare mutation *SRSF2R94\_P95insR*, for these assays. Cells expressing

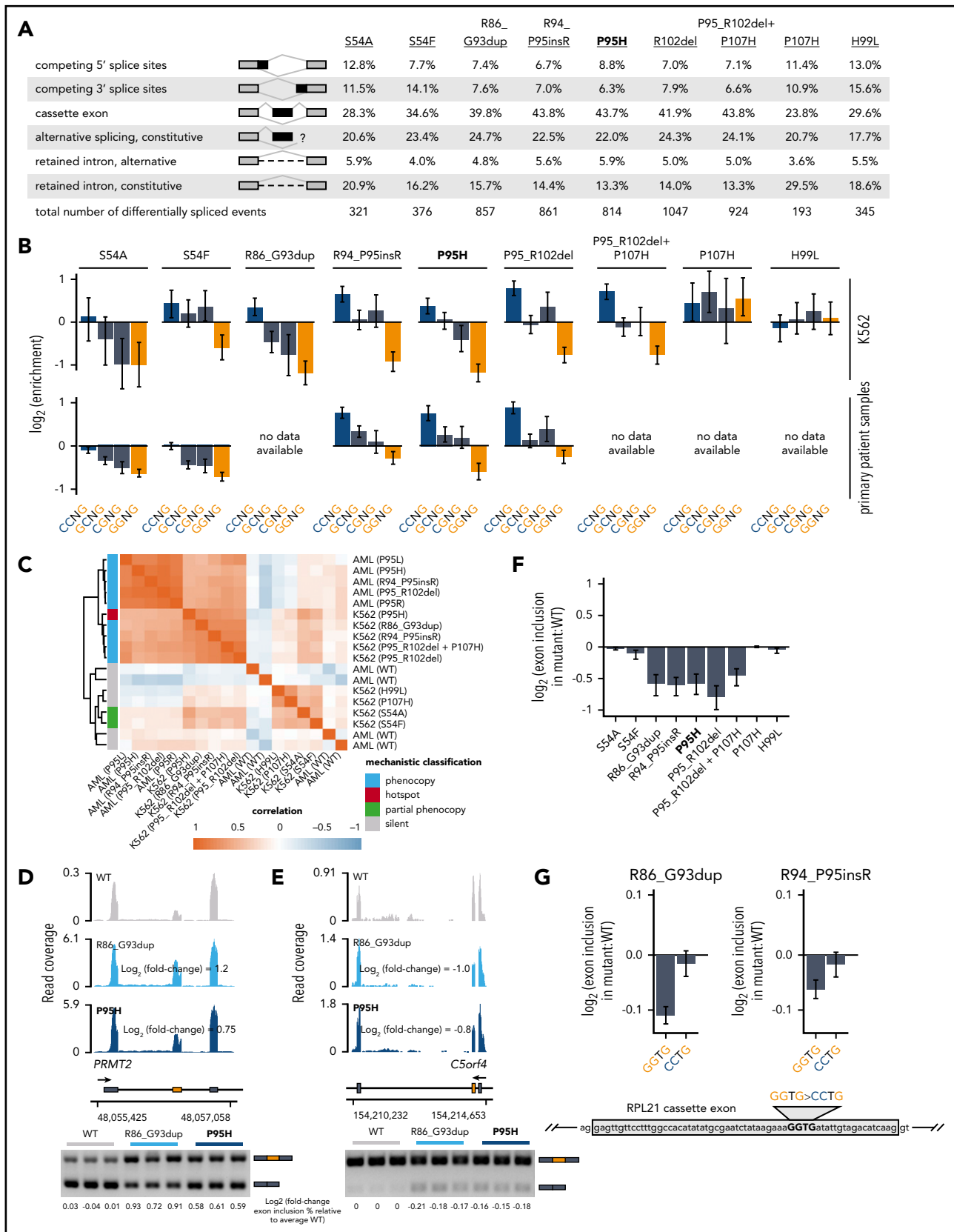


**Figure 2. Rare mutations in *SRSF2* alter exonic splicing enhancer (ESE) preference.** (A) Differentially spliced events identified in K562 cells expressing each indicated *SRSF2* mutant allele relative to WT-expressing control cells. Percentages represent the distribution of differentially spliced events among the indicated event types for each mutation. (B) Enrichment for each indicated variant of the SSNG motif within cassette exons that were promoted vs repressed in cells expressing mutant vs WT *SRSF2*. The enrichment for a given motif was defined as the number of instances in all promoted exons divided by the number of instances in all repressed exons. Error bars

**Table 1. Mechanistic classification of studied mutations**

| Mutation            | n   | Mechanistic classification              | Evidence            | Reference            |
|---------------------|-----|---|---------------------|----------------------|
| <b>SRSF2</b>        |     |   |                     |                      |
| S54A                | 1   | Partial phenocopy of P95                | Cell line + patient | This study           |
| S54F                | 1   | Partial phenocopy of P95                | Cell line + patient | This study           |
| R86_G93dup          | 1   | Phenocopy of P95                        | Cell line           | This study           |
| R94_P95insR         | 11  | Phenocopy of P95                        | Cell line + patient | This study           |
| <b>P95H</b>         | 448 | Hotspot                                 | Cell line + patient | (Previously studied) |
| <b>P95L</b>         | 280 | Hotspot                                 | Cell line + patient | (Previously studied) |
| <b>P95R</b>         | 168 | Hotspot                                 | Cell line + patient | (Previously studied) |
| P95_R102del         | 79  | Phenocopy of P95                        | Cell line + patient | This study           |
| P05_R102del + P107H | 7   | Phenocopy of P95                        | Cell line           | This study           |
| P107H               | 7   | Silent                                  | Cell line           | This study           |
| H99L                | 2   | Silent                                  | Cell line           | This study           |
| <b>U2AF1</b>        |     |   |                     |                      |
| I24T                | 5   | Dual phenocopy of S34 and Q157 (likely) | Cell line + patient | This study           |
| I24V                | 1   | Phenocopy of S34 (likely)               | Cell line           | This study           |
| <b>S34F</b>         | 308 | Hotspot                                 | Cell line + patient | (Previously studied) |
| <b>S34Y</b>         | 92  | Hotspot                                 | Cell line + patient | (Previously studied) |
| R156H               | 30  | Phenocopy of Q157                       | Cell line + patient | This study           |
| R156Q               | 2   | Silent                                  | Cell line           | This study           |
| <b>Q157R</b>        | 66  | Hotspot                                 | Cell line + patient | (Previously studied) |
| <b>Q157P</b>        | 121 | Hotspot                                 | Cell line + patient | (Previously studied) |
| E159_M160insYE      | 8   | Phenocopy of Q157                       | Cell line + patient | This study           |
| S34F + Q157R        | 1   | Dual phenocopy of S34 and Q157          | Cell line           | This study           |

Classification inferred from exonic splicing enhancer preferences and 3' splice site preferences associated with each mutation. The consequences of hotspot (bold) *SRSF2* and *U2AF1* mutations were previously studied by several groups.<sup>20,23,54</sup>

n, number of times that each mutation has been reported in COSMIC.

*SRSF2*R86\_G93dup and *SRSF2*R94\_P95insR both exhibited reduced cassette exon recognition relative to WT cells for the native minigene, as expected, which was abolished by the GGTG>CCTG mutation (Figure 2G). These results confirmed our genomic inference that rare *SRSF2* mutations alter ESE preference and experimentally demonstrate that reduced recognition of G-rich ESEs drives mis-splicing in *SRSF2*-mutant cells.

### Rare *U2AF1* mutations induce both complete and dual phenocopy of altered 3' splice site recognition

Rare *U2AF1* mutations affected a diversity of alternative splicing events as well as a smaller set of normally constitutively spliced introns, with cassette exons exhibiting the most frequent differential splicing (Figure 3A; supplemental Table 3). Unlike *SRSF2* hotspot mutations, which induce identical changes in ESE recognition, *U2AF1* hotspot mutations give rise to 2 distinct changes in RNA-binding specificity and 3' splice site recognition.

*U2AF1*S34F/Y and *Q157P/R* mutations alter sequence-dependent recognition of the nucleotides preceding and after the AG dinucleotide of the 3' splice site, respectively.<sup>23,39,43</sup>

We therefore tested how expression of each rare *U2AF1* mutant allele altered 3' splice site recognition. We identified cassette exons that were differentially spliced in K562 cells expressing each mutant allele relative to WT cells, and computed consensus 3' splice site sequences that were associated with promoted vs repressed cassette exons (Figure 3B; supplemental Figure 3). Expression of the hotspot mutations *U2AF1*S34F and *Q157R* altered recognition of the -3 and +1 sites, as expected. *U2AF1*R156H phenocopied *U2AF1*Q157P/R, as did the rare insertion *U2AF1*E159\_M160insYE. The complex co-mutation *U2AF1*S34F\_Q157R drove a "dual" phenocopy, characterized by S34 and Q157 hotspot-like alterations at both the -3 and +1 positions. The rare mutation *U2AF1*I24T, which affects *U2AF1*'s

**Figure 2 (continued)** represent 95% confidence intervals estimated by bootstrapping. The transcriptomes of patient samples bearing *SRSF2*S54A (polycythemia + hyperleukocytosis + myelofibrosis) and *SRSF2*S54F (chronic myelomonocytic leukemia) were sequenced for this study; RNA-seq data from patient samples bearing *SRSF2*R94\_P95insR (AML), *SRSF2*P95H (chronic myelomonocytic leukemia), and *SRSF2*P95\_R102del (AML) were previously published.<sup>20</sup> (C) Heat map and dendrogram illustrating the global similarity of splicing programs in K562 cells and AML samples expressing the indicated alleles of *SRSF2*. Dendrogram illustrates the results of an unsupervised clustering based on differential splicing in each indicated sample relative to WT-expressing control cells (K562) or a median computed over all WT samples (AML). AML patient data were previously published.<sup>20</sup> (D) RNA-seq read coverage illustrating increased cassette exon inclusion in *PRMT2* in K562 cells expressing either a hotspot (P95H) or private (R86\_G93dup) *SRSF2* mutation (top). Log<sub>2</sub> (fold-change) illustrates log<sub>2</sub> (exon inclusion in mutant- vs WT-expressing cells). RT-PCR validation of RNA-seq results in technical triplicate (bottom). Log fold-changes for RT-PCR computed with respect to the mean signal for WT. (E) As in panel (D), but for a cassette exon in *C5orf4* that is repressed by mutant *SRSF2*. (F) Relative inclusion of a cassette exon within *RPL21* expressed from its endogenous locus in K562 cells expressing mutant vs WT *SRSF2*. Error bars represent 95% confidence intervals for the relative inclusion ratio, computed by propagating the 95% confidence intervals for the 2 isoforms to the ratio for mutant vs WT *SRSF2* by standard rules for error propagation during division of quantities with individual errors. (G) As in panel (F), but where the *RPL21* cassette exon is expressed from a minigene transfected into K562 cells and contains the indicated ESEs. GGTG is the native sequence; CCTG is a mutated ESE that is predicted to be well-recognized in the presence of mutant *SRSF2*. Bars represent the mean ± standard deviation, measured by quantitative RT-PCR and computed over 3 biological replicates.

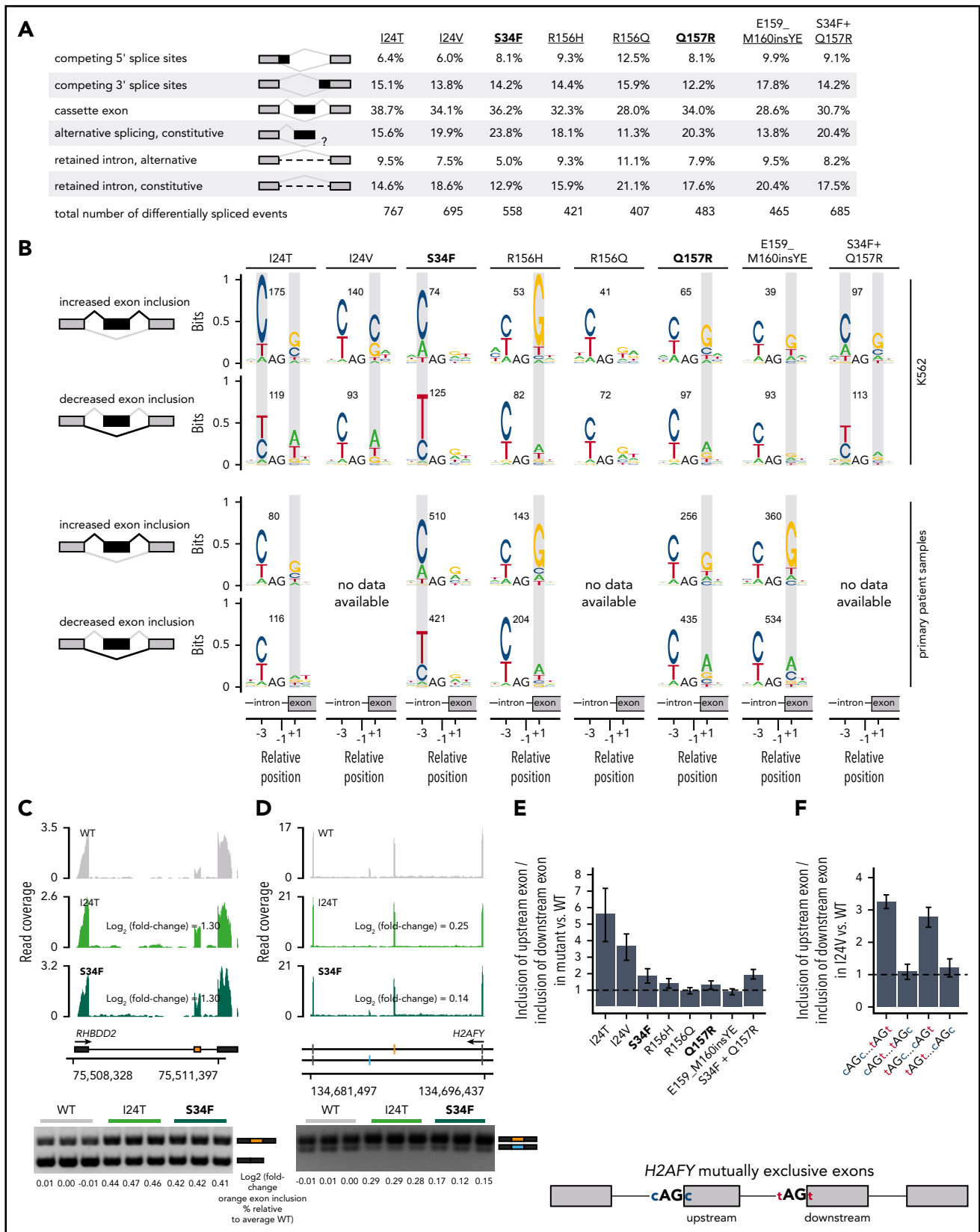


**Figure 3. Rare mutations in *U2AF1* alter 3' splice site recognition.** (A) Differentially spliced events identified in K562 cells expressing each indicated *U2AF1* mutant allele relative to WT-expressing control cells. Percentages represent the distribution of differentially spliced events among the indicated event types for each mutant. (B) Sequence logos representing consensus 3' splice sites of cassette exons that are differentially spliced in K562 cells expressing mutant versus WT *U2AF1*. Gray boxes highlight sequence preferences at the  $-3$  and  $+1$  positions that are similar to those observed in cells expressing the *U2AF1*S34F/Y or *U2AF1*Q157P/R hotspots. RNA-seq data from patient samples bearing *U2AF1*I24T (adrenocortical carcinoma), *U2AF1*S34F (AML), *U2AF1*R156H (myelodysplastic syndromes), *U2AF1*Q157R (AML), and *U2AF1*E159\_M160insYE (AML)

first zinc finger-like S34F/Y, was also associated with a dual phenocopy that was highly similar to that induced by *U2AF1S34F\_Q157R*, whereas *U2AF1I24V* was similar to *U2AF1Q157R* (Table 1). To confirm that these 3' splice site preference alterations were potentially relevant to disease, we extended the above analysis to mutation-matched patient materials. We identified primary patient materials bearing most of the studied rare mutations and compared their transcriptomes with those of WT samples to find similar alterations in consensus 3' splice sites (Figure 3B). For *U2AF1I24T*, we only observed alterations at the +1, and not -3, position, rather than the dual phenocopy that was evident in cell culture, potentially because of the relatively low allelic expression of this mutation in the analyzed patient sample (23% vs 32% allelic expression in the patient samples vs K562 cells expressing *U2AF1I24T*). We used RT-PCR to experimentally validate results from RNA-seq, confirming that *U2AF1I24T* induced similar patterns of mis-splicing, as did *U2AF1S34F* in K562 cells for 4 distinct splicing events (Figure 3C-D; supplemental Figure 5).

We experimentally confirmed that mis-splicing of exons in cells expressing rare *U2AF1* mutations was a direct consequence of altered 3' splice site recognition. We selected a mutually exclusive exon event within *H2AFY* for further study, as *H2AFY* is a robust target of *U2AF1S34F/Y* in both human patients and murine models, whose mis-splicing contributes to impaired hematopoiesis.<sup>23,44,45</sup> Similar to *U2AF1S34F*, the rare mutations *U2AF1I24T/V* promoted upstream exon inclusion while repressing downstream exon inclusion (Figure 3E). We cloned *H2AFY*'s mutually exclusive exons and flanking introns and exons into a minigene cassette and created mutant versions of the minigene, where we mutated the 3' splice sites of both mutually exclusive exons as follows: swap the nucleotides at the -3 positions, swap the nucleotides at the +1 positions, and swap the nucleotides at both the -3 and +1 positions. We transfected these minigenes into WT and *U2AF1I24V* cells, where we focused on *U2AF1I24V*, as we were unable to obtain patient samples bearing this lesion for transcriptome analysis, and measured relative levels of upstream vs downstream exon inclusion. These experiments revealed that native C and T at the +1 positions of the upstream and downstream exons were both essential for mutation-dependent splicing, whereas the nucleotides at the -3 positions could be swapped without consequence (Figure 3F). These minigene experiments confirm our genomic inference that *U2AF1I24V* induces *H2AFY* mis-splicing by altering recognition of the +1 position of the 3' splice sites of both of *H2AFY*'s mutually exclusive exons.

### Mechanistic classification of mutations explains extent of transcriptome dysregulation

Our analyses of ESE and 3' splice site recognition in *SRSF2*- and *U2AF1*-mutant cells and patient materials clearly distinguished between mutations that did or did not alter the normal functions of *SRSF2* and *U2AF1* (Table 1). Although hotspot *SRSF2* and

*U2AF1* mutations induce distinctive mis-splicing programs that contribute to disease phenotypes, they have also been shown to affect other cellular processes of potential disease relevance including mRNA translation<sup>46</sup> and R loop formation.<sup>47,48</sup> We reasoned that if a given rare mutation altered a critical cellular process, then that alteration might be reflected in dysregulated gene expression relative to WT cells. This hypothesis is consistent with previous observations that many cancer-causing mutations that act through diverse molecular pathways induce stereotyped and readily detectable alterations in gene expression profiles.<sup>29</sup> We therefore compared the extent of gene expression vs splicing dysregulation to find that hotspot and rare mutations that phenocopied hotspot mutations induced dramatic changes in gene expression, whereas putative passenger mutations with no apparent effects on ESE or 3' splice site recognition similarly had few effects on global gene expression (Figure 4A-B; supplemental Tables 4 and 5). This analysis supports, although does not prove, our hypothesis that rare *SRSF2* or *U2AF1* mutations that do not alter ESE or 3' splice site recognition are likely functionally silent passengers.

### Rare *SRSF2* and *U2AF1* mutations converge on a small set of disease-relevant events

Although *SRSF2* and *U2AF1* mutations induce distinct alterations in RNA splicing, we wondered whether they might converge on shared downstream targets that contribute to their enrichment in hematologic disease. We speculated that such targets might exhibit concordant differential splicing in association with both hotspot and rare mutations. We therefore identified cassette and mutually exclusive exons within coding genes that were differentially spliced in association with at least 3 of the 5 *SRSF2P95*-like mutations and compared that set with differentially spliced exons found in association with 3 of the *U2AF1S34*-like mutations. As expected, given *SRSF2* and *U2AF1* mutations' distinct consequences for splicing, as well as these lesions' preferential enrichment in different disease subtypes,<sup>1,49</sup> the vast majority of differentially spliced exons were *SRSF2*- or *U2AF1*-specific. However, 3 genes were differentially spliced in association with both *SRSF2* and *U2AF1* mutations (Figure 4C), of which *H2AFY* and *IRAK4* were particularly notable, given their known involvement in hematologic disease. Previous studies demonstrated that *U2AF1S34F/Y* promotes inclusion of the upstream exon of 2 mutually exclusive exons within *H2AFY*, which encodes macro-H2A1, thereby perturbing erythroid and granulomonocytic differentiation.<sup>23,44,45</sup> *U2AF1S34F* similarly promotes inclusion of an *IRAK4* cassette exon to drive the *IRAK4*-long isoform that activates innate immune signaling and is important for leukemic cell function<sup>24</sup> (Figure 4D). Our analysis revealed that the rare mutations *U2AF1I24T/V* phenocopied the *H2AFY* and *IRAK4* mis-splicing characteristic of *U2AF1S34F/Y*-mutant cells, and furthermore, that both *SRSF2P95* and *SRSF2P95*-like mutations drove *H2AFY*, as well as *IRAK4* differential splicing

**Figure 3 (continued)** were previously published.<sup>34-37</sup> (C) RNA-seq read coverage illustrating increased cassette exon inclusion in *RHBDD2* in K562 cells expressing either a hotspot (S34F) or rare (I24T) *U2AF1* mutation (top). Log<sub>2</sub> (fold-change) illustrates log<sub>2</sub> (exon inclusion in mutant- vs WT-expressing cells). RT-PCR validation of RNA-seq results in technical triplicate (bottom). Log fold-changes for RT-PCR computed with respect to the mean signal for WT. (D) As panel C, but for mutually exclusive exons in *H2AFY*. The upstream (orange) exon is the exon for which inclusion is calculated. (E) Relative inclusion of the upstream vs downstream exon for 2 mutually exclusive exons within *H2AFY* expressed from its endogenous locus in K562 cells expressing mutant versus WT *U2AF1* as estimated by RNA-seq. Error bars represent 95% confidence intervals for the relative inclusion ratio, computed by propagating the 95% confidence intervals for the 2 isoforms to the ratio for mutant vs WT *SRSF2* by standard rules for error propagation during division of quantities with individual errors. (F) As in panel (E), but where the *H2AFY* mutually exclusive exons are expressed from a minigene transfected into K562 cells and contain 3' splice sites with the indicated sequences. AG is the AG dinucleotide of the 3' splice site. Bars represent the mean ratio of inclusion of the upstream:downstream exons ± standard deviation, estimated by quantitative RT-PCR and computed over 3 biological replicates.



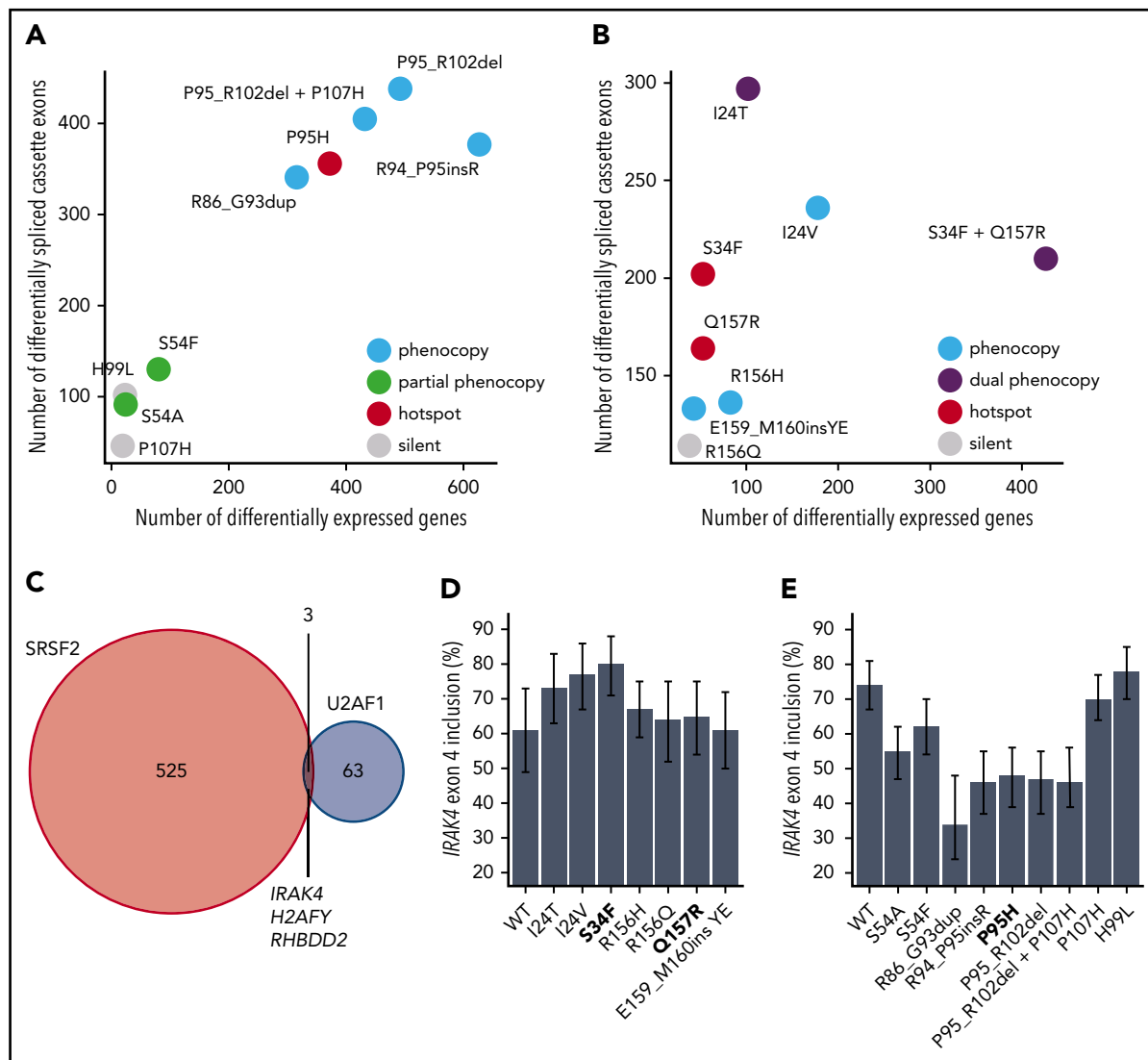


**Figure 4. Hotspot and rare *SRSF2* and *U2AF1* induce transcriptome dysregulation and converge on *H2AFY* and *IRAK4* mis-splicing.** (A) Scatter plot comparing the numbers of differentially expressed genes (x-axis) and differentially spliced cassette exons (y-axis) in K562 cells expressing each indicated *SRSF2* mutation vs WT-expressing control cells. Differentially expressed genes were defined as those genes with expression at least 1 TPM in both samples,  $|\log_2(\text{fold-change})| \geq \log_2(1.5)$ , and Bayes factor at least 10. See Table 1 for additional information on classification of each mutation. (B) As panel A, but for the indicated *U2AF1* mutations. (C) Venn diagram illustrating the sets of coding genes containing cassette exons and mutually exclusive exons that were differentially spliced in association with both hotspot and rare *SRSF2* and/or *U2AF1* mutations relative to control WT-expressing cells. Differentially spliced exons were defined as those exhibiting a change in isoform ratio at least 10% and a Bayes factor at least 1. Diagram restricted to genes containing cassette exons or mutually exclusive exons that were differentially spliced in association with at least 3 *SRSF2*P95-like mutations (*SRSF2*R86\_G93dup, *SRSF2*R94\_P95insR, *SRSF2*P95H, *SRSF2*P95\_R102del, and *SRSF2*P95\_R102del + P107H considered) and 3 *U2AF1*S34-like mutations (*U2AF1*I24T, *U2AF1*I24V, and *U2AF1*S34F considered). (D) Inclusion of a cassette exon within *IRAK4* in K562 cells expressing each indicated *U2AF1* allele. Error bars represent 95% confidence intervals as estimated by MISO.<sup>55</sup> (E) As in panel (D), but for cells expressing each indicated *SRSF2* allele.

(Figure 4C; supplemental Table 1). Intriguingly, however, *SRSF2* mutations drove *H2AFY* and *IRAK4* mis-splicing that was in direct opposition to that caused by *U2AF1* mutations (Figure 4E; supplemental Table 3). As 2 of the 3 coding genes that are shared targets of both hotspot and rare *SRSF2* and *U2AF1* mutations have been previously implicated in the pathology of *U2AF1*-mutant cells, we speculate that differential splicing of *H2AFY* and *IRAK4* may be similarly important for the functional consequences of *SRSF2* mutations.

## Discussion

In addition to characterizing the function of rare mutations in *SRSF2* and *U2AF1*, our study illustrates a method for inferring

mutational pathogenicity when a biological assay such as tumorigenesis is inaccessible. Although *SRSF2* and *U2AF1* mutations exhibit the genetic enrichment expected of driver lesions in many dysplastic and neoplastic disorders, they do not confer a growth advantage to cultured transformed cells and are dispensable for the maintenance of at least some xenografts.<sup>20,23,39,50</sup> We therefore took advantage of the stereotyped changes in RNA splicing caused by *SRSF2* and *U2AF1* hotspot mutations, which have been directly linked to disease phenotypes,<sup>20-24</sup> to classify rare mutations as candidate drivers or passengers. Although unbiased cluster analyses (Figure 1F-G) separated mutations similarly to subsequent mechanism-based analyses, only the latter can classify pathogenicity with reasonable confidence, given the known role of dysfunctional exon and

splice site recognition in *SRSF2*- and *U2AF1*-mutant hematologic malignancies.

Our approach can confidently identify functionally active *SRSF2* and *U2AF1* mutations that alter ESE or 3' splice site recognition, but cannot prove that any given mutation is functionally silent. Many cancer driver mutations directly or indirectly dysregulate gene expression, irrespective of the means by which they promote cancer, in a specific manner.<sup>29</sup> Therefore, the concordance between our classification of mutations and the extent of transcriptome dysregulation that each induces (Figure 4A-B) suggests that *SRSF2* and *U2AF1* mutations that do not detectably alter exon or splice site recognition are likely passengers. However, we cannot rule out the possibility that some rare mutations promote disease through means that are undetectable via transcriptomic analyses. For example, recent studies have reported increased R loop formation in cells expressing *SRSF2* and *U2AF1* hotspot mutations (although a causative role for R loop formation in dysplastic hematopoiesis or tumorigenesis has not yet been demonstrated).<sup>47,48</sup> Conversely, although our approach accurately tests whether individual rare mutations induce molecular phenocopies of pathogenic hotspot mutations, it only provides a likely estimate (not proof) of pathogenicity. Even variants that we classify as likely pathogenic should be interpreted with care and caution in a clinical setting.

A published structure of *SRSF2*<sup>51</sup> offers insight into the potential means by which rare and hotspot mutations cause convergent splicing alterations (supplemental Figure 6). Rare mutations affecting the P95 hotspot presumably induce a similar set of domain movements as those induced by *SRSF2*P95H/L/R,<sup>20</sup> whereas S54 lies distal to the binding core, and so likely affects RNA binding indirectly. H99 interacts with the variable nucleotide in the CCNG motif, potentially explaining why *SRSF2*H99L did not induce detectable changes in ESE preference.

Our study has several implications for basic and translational studies of spliceosomal mutations. First, as many rare *SRSF2* and *U2AF1* mutations generate molecular phenocopies of the *SRSF2*P95, *U2AF1*S34, and *U2AF1*Q157 hotspot mutations, studying those hotspot mutations will also give insight into the pathology of diverse rarer mutations. Second, because rare and even private *SRSF2* and *U2AF1* mutations may be pathogenic, non-hotspot mutations should be considered in early detection and monitoring studies<sup>15</sup> when feasible. Finally, when therapies designed to specifically target cells with spliceosomal mutations enter clinical practice,<sup>38,40,52,53</sup> patients bearing non-hotspot spliceosomal mutations should be considered as candidates for these therapies. Although performing a whole-transcriptome analysis is not feasible in a clinical setting, continued study of both hotspot and hotspot-phenocopy mutations may reveal specific biomarkers of mutant *SRSF2* and *U2AF1* activity that can

be used to rapidly classify novel spliceosomal mutations as drivers or passengers for precision medicine.

## Acknowledgments

The results shown here are in part based upon data generated by the TCGA Research Network: <https://cancergenome.nih.gov/>. This research was supported, in part, by the National Institutes of Health (NIH)/National Institute of Diabetes and Digestive and Kidney Diseases (R01 DK103854; R.K.B.), NIH/National Heart, Lung, and Blood Institute (R01 HL128239; R.K.B. and O.A.-W.), the Department of Defense Bone Marrow Failure Research Program (W81XWH-16-1-0059; R.K.B. and O.A.-W.), the EvansS Foundation (R.K.B. and O.A.-W.), the Henry & Marilyn Taub Foundation (O.A.-W.), and the NIH/National Cancer Institute (P30 CA015704; Genomics Shared Resources of the Fred Hutch/University of Washington Cancer Consortium). J.T. is supported by the Conquer Cancer Foundation of the American Society of Clinical Oncology, the American Association for Cancer Research, the American Society of Hematology, the Robert Wood Johnson Foundation, and the NIH/National Cancer Institute (K08 CA230319). O.A.-W. is supported by the Pershing Square Sohn Cancer Research Alliance. R.K.B. is a scholar of the Leukemia & Lymphoma Society (1344-18).

## Authorship

Contribution: J.P. performed experiments and computational analyses; J.P. and R.K.B. wrote the paper; J.-J.K., B.C., A.R., J.T., and O.A.-W. provided patient material; and J.T.P. and K.N. contributed to data interpretation.

Conflict-of-interest disclosure: O.A.-W. has served as a consultant for H3 Biomedicine, Foundation Medicine Inc, Merck, and Janssen, serves on the Scientific Advisory Board of Envisagenics Inc, and has received prior research funding from H3 Biomedicine unrelated to the current manuscript.

ORCID profiles: J.P., 0000-0002-6046-614X; J.-J.K., 0000-0002-8121-438X; B.C., 0000-0002-6514-3905; J.T., 0000-0003-4407-6325; J.T.P., 0000-0001-6570-1789; O.A.-W., 0000-0002-3907-6171; R.K.B., 0000-0002-8046-1063.

Correspondence: Robert K. Bradley, 1100 Fairview Ave N, Seattle, WA 98109; e-mail: rbradley@fredhutch.org.

## Footnotes

Submitted 14 August 2019; accepted 8 January 2020; prepublished online on *Blood* First Edition 21 January 2020. DOI 10.1182/blood.2019002894.

Other data that support this study's findings are available from the authors upon reasonable request.

The online version of this article contains a data supplement.

There is a *Blood* Commentary on this article in this issue.

The publication costs of this article were defrayed in part by page charge payment. Therefore, and solely to indicate this fact, this article is hereby marked "advertisement" in accordance with 18 USC section 1734.

## REFERENCES

1. Yoshida K, Sanada M, Shiraishi Y, et al. Frequent pathway mutations of splicing machinery in myelodysplasia. *Nature*. 2011;478(7367):64-69.
2. Graubert TA, Shen D, Ding L, et al. Recurrent mutations in the *U2AF1* splicing factor in myelodysplastic syndromes. *Nat Genet*. 2011; 44(1):53-57.
3. Papaemmanuil E, Cazzola M, Boulton J, et al; Chronic Myeloid Disorders Working Group of the International Cancer Genome Consortium. Somatic SF3B1 mutation in myelodysplasia with ring sideroblasts. *N Engl J Med*. 2011;365(15): 1384-1395.
4. Visconte V, Makishima H, Jankowska A, et al. SF3B1, a splicing factor is frequently mutated in refractory anemia with ring sideroblasts. *Leukemia*. 2012;26(3):542-545.
5. Wang L, Lawrence MS, Wan Y, et al. SF3B1 and other novel cancer genes in chronic lymphocytic leukemia. *N Engl J Med*. 2011; 365(26):2497-2506.
6. Quesada V, Conde L, Villamor N, et al. Exome sequencing identifies recurrent mutations of

- the splicing factor SF3B1 gene in chronic lymphocytic leukemia. *Nat Genet.* 2011;44(1):47-52.
7. Dvinge H, Kim E, Abdel-Wahab O, Bradley RK. RNA splicing factors as oncoproteins and tumour suppressors. *Nat Rev Cancer.* 2016;16(7):413-430.
  8. Seiler M, Peng S, Agrawal AA, et al; Cancer Genome Atlas Research Network. Somatic Mutational Landscape of Splicing Factor Genes and Their Functional Consequences across 33 Cancer Types. *Cell Reports.* 2018;23(1):282-296.
  9. Rossi D, Brusca G, Spina V, et al. Mutations of the SF3B1 splicing factor in chronic lymphocytic leukemia: association with progression and fludarabine-refractoriness. *Blood.* 2011;118(26):6904-6908.
  10. Ramsay AJ, Rodríguez D, Villamor N, et al. Frequent somatic mutations in components of the RNA processing machinery in chronic lymphocytic leukemia. *Leukemia.* 2013;27(7):1600-1603.
  11. Yoshimi A, Lin K-T, Wiseman DH, et al. Coordinated alterations in RNA splicing and epigenetic regulation drive leukaemogenesis. *Nature.* 2019;574(7777):273-277.
  12. Martin M, Maßhöfer L, Temming P, et al. Exome sequencing identifies recurrent somatic mutations in EIF1AX and SF3B1 in uveal melanoma with disomy 3. *Nat Genet.* 2013;45(8):933-936.
  13. Harbour JW, Roberson EDO, Anbunathan H, Onken MD, Worley LA, Bowcock AM. Recurrent mutations at codon 625 of the splicing factor SF3B1 in uveal melanoma. *Nat Genet.* 2013;45(2):133-135.
  14. Abelson S, Collord G, Ng SWK, et al. Prediction of acute myeloid leukaemia risk in healthy individuals. *Nature.* 2018;559(7714):400-404.
  15. Desai P, Mencia-Trinchant N, Savenkov O, et al. Somatic mutations precede acute myeloid leukemia years before diagnosis. *Nat Med.* 2018;24(7):1015-1023.
  16. DeBoever C, Ghia EM, Shepard PJ, et al. Transcriptome sequencing reveals potential mechanism of cryptic 3' splice site selection in SF3B1-mutated cancers. *PLOS Comput Biol.* 2015;11(3):e1004105.
  17. Darman RB, Seiler M, Agrawal AA, et al. Cancer-associated SF3B1 hotspot mutations induce cryptic 3' splice site selection through use of a different branch point. *Cell Reports.* 2015;13(5):1033-1045.
  18. Alsafadi S, Houy A, Battistella A, et al. Cancer-associated SF3B1 mutations affect alternative splicing by promoting alternative branchpoint usage. *Nat Commun.* 2016;7(1):10615.
  19. Inoue D, Chew G-L, Liu B, et al. Spliceosomal disruption of the non-canonical BAF complex in cancer. *Nature.* 2019;574(7778):432-436.
  20. Kim E, Ilagan JO, Liang Y, et al. SRSF2 Mutations Contribute to Myelodysplasia by Mutant-Specific Effects on Exon Recognition. *Cancer Cell.* 2015;27(5):617-630.
  21. Zhang J, Lieu YK, Ali AM, et al. Disease-associated mutation in SRSF2 misregulates splicing by altering RNA-binding affinities. *Proc Natl Acad Sci U S A.* 2015;112(34):E4726-E4734.
  22. Brooks AN, Choi PS, de Waal L, et al. A pan-cancer analysis of transcriptome changes associated with somatic mutations in U2AF1 reveals commonly altered splicing events [published correction appears in *PLoS One* 9(4):e96437]. *PLoS One.* 2014;9(1):e87361.
  23. Ilagan JO, Ramakrishnan A, Hayes B, et al. U2AF1 mutations alter splice site recognition in hematological malignancies. *Genome Res.* 2015;25(1):14-26.
  24. Smith MA, Choudhary GS, Pellagatti A, et al. U2AF1 mutations induce oncogenic IRAK4 isoforms and activate innate immune pathways in myeloid malignancies. *Nat Cell Biol.* 2019;21(5):640-650.
  25. Tate JG, Bamford S, Jubb HC, et al. COSMIC: the catalogue of somatic mutations in cancer. *Nucleic Acids Res.* 2019;47(D1):D941-D947.
  26. Starita LM, Young DL, Islam M, et al. Massively parallel functional analysis of BRCA1 RING domain variants. *Genetics.* 2015;200(2):413-422.
  27. Starita LM, Islam MM, Banerjee T, et al. A multiplex homology-directed DNA repair assay reveals the impact of more than 1,000 BRCA1 missense substitution variants on protein function. *Am J Hum Genet.* 2018;103(4):498-508.
  28. Findlay GM, Daza RM, Martin B, et al. Accurate classification of BRCA1 variants with saturation genome editing. *Nature.* 2018;562(7726):217-222.
  29. Berger AH, Brooks AN, Wu X, et al. High-throughput phenotyping of lung cancer somatic mutations [published correction appears in *Cancer Cell.* 2017;32(6):884]. *Cancer Cell.* 2016;30(2):214-228.
  30. Kim E, Ilic N, Shrestha Y, et al. Systematic functional interrogation of rare cancer variants identifies oncogenic alleles. *Cancer Discov.* 2016;6(7):714-726.
  31. Agrawal AA, Seiler M, Brinton LT, et al. Novel SF3B1 in-frame deletions result in aberrant RNA splicing in CLL patients. *Blood Adv.* 2017;1(15):995-1000.
  32. Wagenmakers E-J, Lodewyckx T, Kuriyal H, Grasman R. Bayesian hypothesis testing for psychologists: a tutorial on the Savage-Dickey method. *Cognit Psychol.* 2010;60(3):158-189.
  33. Durham BH, Getta B, Dietrich S, et al. Genomic analysis of hairy cell leukemia identifies novel recurrent genetic alterations. *Blood.* 2017;130(14):1644-1648.
  34. Pellagatti A, Armstrong RN, Steeples V, et al. Impact of spliceosome mutations on RNA splicing in myelodysplasia: dysregulated genes/pathways and clinical associations. *Blood.* 2018;132(12):1225-1240.
  35. Lavallée V-P, Baccelli I, Kros J, et al. The transcriptomic landscape and directed chemical interrogation of MLL-rearranged acute myeloid leukemias. *Nat Genet.* 2015;47(9):1030-1037.
  36. Zheng S, Cherniack AD, Dewal N, et al; Cancer Genome Atlas Research Network. Comprehensive pan-genomic characterization of adrenocortical carcinoma [published correction appears in *Cancer Cell.* 2016;30(2):363]. *Cancer Cell.* 2016;29(5):723-736.
  37. Ley TJ, Miller C, Ding L, et al; Cancer Genome Atlas Research Network. Genomic and epigenomic landscapes of adult de novo acute myeloid leukemia. *N Engl J Med.* 2013;368(22):2059-2074.
  38. Lee SC-W, Dvinge H, Kim E, et al. Modulation of splicing catalysis for therapeutic targeting of leukemia with mutations in genes encoding spliceosomal proteins. *Nat Med.* 2016;22(6):672-678.
  39. Fei DL, Motowski H, Chatrikhi R, et al. Wild-type U2AF1 antagonizes the splicing program characteristic of U2AF1-mutant tumors and is required for cell survival. *PLoS Genet.* 2016;12(10):e1006384.
  40. Shirai CL, White BS, Tripathi M, et al. Mutant U2AF1-expressing cells are sensitive to pharmacological modulation of the spliceosome. *Nat Commun.* 2017;8(1):14060.
  41. Dvinge H, Bradley RK. Widespread intron retention diversifies most cancer transcriptomes. *Genome Med.* 2015;7(1):45.
  42. Liang Y, Tebaldi T, Rejeski K, et al. SRSF2 mutations drive oncogenesis by activating a global program of aberrant alternative splicing in hematopoietic cells. *Leukemia.* 2018;32(12):2659-2671.
  43. Okeyo-Owuor T, White BS, Chatrikhi R, et al. U2AF1 mutations alter sequence specificity of pre-mRNA binding and splicing. *Leukemia.* 2015;29(4):909-917.
  44. Shirai CL, Ley JN, White BS, et al. Mutant U2AF1 expression alters hematopoiesis and Pre-mRNA splicing in vivo. *Cancer Cell.* 2015;27(5):631-643.
  45. Yip BH, Steeples V, Repapi E, et al. The U2AF1S34F mutation induces lineage-specific splicing alterations in myelodysplastic syndromes. *J Clin Invest.* 2017;127(6):2206-2221.
  46. Palangat M, Anastasakis DG, Fei DL, et al. The splicing factor U2AF1 contributes to cancer progression through a noncanonical role in translation regulation. *Genes Dev.* 2019;33(9-10):482-497.
  47. Chen L, Chen J-Y, Huang Y-J, et al. The augmented R-loop is a unifying mechanism for myelodysplastic syndromes induced by high-risk splicing factor mutations. *Mol Cell.* 2018;69(3):412-425.
  48. Nguyen HD, Leong WY, Li W, et al. Spliceosome mutations induce R loop-associated sensitivity to ATR inhibition in myelodysplastic syndrome. *Cancer Res.* 2018;78(18):5363-5374.
  49. Haferlach T, Nagata Y, Grossmann V, et al. Landscape of genetic lesions in 944 patients with myelodysplastic syndromes. *Leukemia.* 2014;28(2):241-247.
  50. Fei DL, Zhen T, Durham B, et al. Impaired hematopoiesis and leukemia development in mice with a conditional knock-in allele of a mutant splicing factor gene *U2af1*. *Proc Natl Acad Sci USA.* 2018;115(44):E10437-E10446.

51. Daubner GM, Cléry A, Jayne S, Stevenin J, Allain FH. A syn-anti conformational difference allows SRSF2 to recognize guanines and cytosines equally well. *EMBO J*. 2012;31(1):162-174.
52. Obeng EA, Chappell RJ, Seiler M, et al. Physiologic expression of Sf3b1(K700E) causes impaired erythropoiesis, aberrant splicing, and sensitivity to therapeutic spliceosome modulation. *Cancer Cell*. 2016;30(3):404-417.
53. Seiler M, Yoshimi A, Darman R, et al. H3B-8800, an orally available small-molecule splicing modulator, induces lethality in spliceosome-mutant cancers. *Nat Med*. 2018;24(4):497-504.
54. Przychodzen B, Jerez A, Guinta K, et al. Patterns of missplicing due to somatic U2AF1 mutations in myeloid neoplasms. *Blood*. 2013;122(6):999-1006.
55. Katz Y, Wang ET, Airolidi EM, Burge CB. Analysis and design of RNA sequencing experiments for identifying isoform regulation. *Nat Methods*. 2010;7(12):1009-1015.